Put a Ring on It: Improving the Thermal Stability of Molybdenum Imides Through Ligand Rigidification

Michael A. Land,*,# Kieran G. Lawford, Lara K. Watanabe, Marshall Atherton, and Seán T. Barry

Department of Chemistry, Carleton University, Ottawa, Ontario, K1S 5B6, Canada

Supporting Information Placeholder

ABSTRACT: Volatile bis(*tert*-butylimido)-dichloromolybdenum(VI) compounds containing *N,N'*-chelating ligands, (^{t}BuN)$_2$MoCl$_2$·L, have previously been used as single-source precursors for the chemical vapor deposition of high-purity Mo_2N thin films. The first step in the thermolysis of these compounds is the partial dissociation of the chelating ligand to yield (^{t}BuN)$_2$MoCl$_2$, which further decomposes by eliminating isobutylene and ^{t}BuNH$_2$. The rate determining step in this process is the formation of a pentacoordinate intermediate where the previously bidentate ligand adopts a κ_1-coordination. Here we show that rigidification of the ligand backbone, by incorporating various heterocycles, led to an overall increase in thermal stability (21−38 °C) of these complexes by preventing the formation of the κ_1-intermediate. Formation of the κ_1-intermediates is highlighted by high level calculations and is supported by experimental activation barriers. Finally, a model for the κ_1-bipyridine adduct was isolated and characterized using 2-phenylpyridine. This careful control of the thermal stabilities of these compounds can lead to new vapor-phase deposition precursors for the preparation of Mo_2N films.

The design of new vapor phase deposition precursors often relies on understanding a compound's mechanism(s) of thermal decomposition.[1–7] These processes must be understood to determine if a compound can produce thin films that contain desirable material properties. Insights into these decomposition pathways can also be used to fine-tune precursors by designing, and incorporating, new ligand scaffolds that block these primary decomposition pathways, or by making them kinetically inaccessible.[1–8] This can lead to an overall improvement to the thermal stability of precursors, making them viable at higher temperatures for the deposition of ultrahigh purity thin films.

For example, one of the most common ligand classes used in precursors for the vapor-deposition of thin metal films, amidinates,[2,9] have had several "redesigns,"[1–5,10] each of which has led to an overall improvement to the thermal stability of the precursor compounds (**Figure 1**). First, replacement of the *N,N'*-diisopropyl groups (**A**) with *tert*-butyl groups (**B**) resulted in thermal enhancement by removing the β-H decomposition pathway;[3,4] β-Me migrations have a higher barrier. Amidinate ligands can also decompose through carbodiimide (CDI) de-insertion reactions,[1,2,11] which often result in methylated complexes (*e.g.*, M−Me) and the dissociation of a CDI molecule. This issue was addressed by our group by using an imino-pyrrolidine (**C**) which appends the central carbon atom to a heterocycle containing the chelating nitrogen atom, in turn making CDI de-insertion inaccessible.[1]

The imino-pyrrolidine ligand (**C**) is monocyclic, and therefore the β-Me groups of the exocyclic *tert*-butylimino moiety are still accessible to potential β-Me migrations, through a postulated monodentate intermediate.[5] Gordon *et al.* have addressed this by preparing rigid 5,5-bicyclic amidine ligands (**D**).[5] The added rigidity provided by this new ligand constrained the ligand in the metal complex, preventing it from isomerizing to a monodentate intermediate. Therefore, potential β-Me decomposition pathways need to proceed through strained, higher energy, transition states, which resulted in an improvement to the thermal stability of complexes that incorporate **D**.[5]

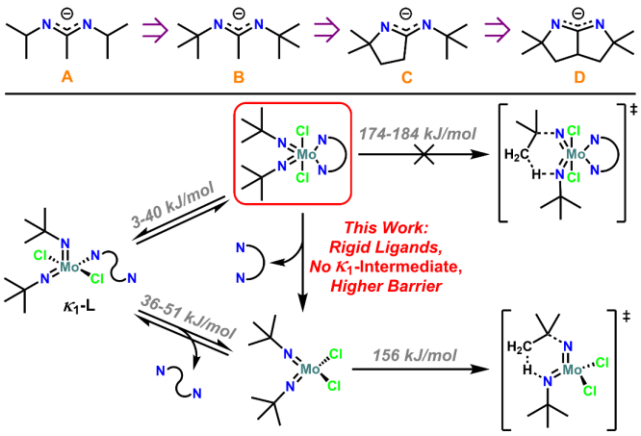

Figure 1. Example of ligand engineering used for vapor-phase deposition precursors (top). Simplified mechanism for the thermal decomposition of (^{t}BuN)$_2$MoCl$_2$·L compounds (L = neutral *N,N'*-chelating ligand) (bottom). Thermodynamic values obtained from reference 6.

This concept of "tethering" two sides of a chelating ligand together, to prevent the formation of monodentate intermediates, piqued our interest as a facile method to improve the thermal stability of known vapor deposition precursors, without drastically changing the electronics or reactivity at the metal center. Here we report a redesign of the (^{t}BuN)$_2$MoCl$_2$·L (L = neutral,

N,N'-chelating ligand) class of compounds that we have recently used as precursors for the single-source CVD of high quality Mo_2N thin films.[7] We have previously shown that these compounds undergo thermal decomposition by first losing their neutral chelating ligand (**Figure 1**),[6,12] leading to the generation of $(^tBuN)_2MoCl_2$, which was isolated as $[(^tBuN)Mo(\mu\text{-}N^tBu)Cl_2]_2$ in the solid state.[13] $(^tBuN)_2MoCl_2$ then undergoes an irreversible γ-H migration to yield isobutylene and $(^tBuHN)MoNCl_2$.[6,12]

As a finer detail to this mechanism, we found that the neutral chelating ligands first undergo a low energy isomerization to yield a pentacoordinate, κ_1-complex (**Figure 1**).[6] This intermediate then loses its ligand to yield $(^tBuN)_2MoCl_2$, which subsequently undergoes thermal decomposition; a phenomenon that was supported by experimental and computational results.[6] As an additional note, we have previously redesigned the general $(RN)_2MoCl_2$ framework, focusing on the effect of the alkyl imido ligands (*e.g.*, R = *tert*-pentyl, *tert*-octyl, 1-adamantyl, and a cyclic imido from 2,5-dimethylhexane-2,5-diamine) and found that all those compounds follow a similar decomposition mechanism as outlined above.[12]

Recently we described the synthesis and thermal stability of the 2,2'-bipyridine (bpy) adduct of $(^tBuN)_2MoCl_2$, **1a** (**Figure 2**).[6,12,13] This compound exhibited good thermal stability, and its onset of thermal decomposition (T_D) was found to be 272 °C. Similarly, the 1,10-phenanthroline (phen) adduct of $(^tBuN)_2MoCl_2$, **1b**, exhibited excellent thermal stability with a T_D of 303 °C.[6,12] We speculated that the improved thermal stability of **1b** over **1a** might be due to the rigidity of phen. Notably, the bpy ligand in **1a** is capable of rotating around its C−C bond to yield a pentacoordinate κ_1-intermediate (**Figure 1**), whereas phen cannot undergo this rotation. Therefore, we decided to prepare rigid analogues of other *N,N'*-chelating ligands that we previously investigated, to further investigate the effect of ligand rigidification.

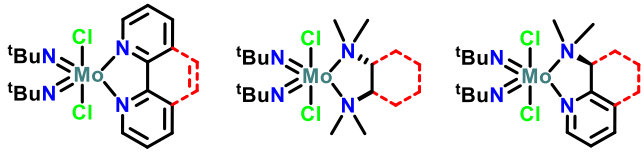

Figure 2. Structures of the $(^tBuN)_2MoCl_2$·L compounds used herein. The red dashed bonds highlight where the *N,N'*-chelates were rigidified.

We began this investigation by using *(1S, 2S)*-*N,N,N',N'*-tetramethylcyclohexane-1,2-diamine (tmchd), which is a commercially available, rigid analogue of *N,N,N',N'*-tetramethyl-ethylenediamine (tmeda). Treatment of tmchd with a pentane solution of $(^tBuN)_2MoCl_2$·dme[14] led to the precipitation of $(^tBuN)_2MoCl_2$·tmchd (**2b**, **Figure 2**), in high yield (see SI for experimental details). The structure of **2b** was confirmed using NMR spectroscopy, which revealed two N*Me*$_2$ environments (*i.e.*, $N(CH_3)_A(CH_3)_B$) by both ^1H and ^{13}C NMR spectroscopy, due to the different methyl environments arising from the enantiospecific ligand. The proposed formula of **2b** was also confirmed using combustion analysis.

We then synthesized a new ligand, *N,N*-dimethyl-5,6,7,8-tetrahydoquinolin-8-amine (dmthqa), by the Eschweiler-Clarke methylation[15] of 5,6,7,8-tetrahdroquinolin-8-amine using formic acid and paraformaldehyde; dmthqa is a rigid analogue of 2-(*N,N*-dimethylamino)methylpyridine (dmampy). The structure of the new ligand was confirmed by ^1H NMR spectroscopy and high-resolution electrospray ionization mass spectrometry. Direct treatment of dmthqa with an ethereal solution of $(^tBuN)_2MoCl_2$·dme led to the isolation of $(^tBuN)_2MoCl_2$·dmthqa (**3b**, **Figure 2**). Again, two inequivalent N*Me*$_2$ signals were observed by both ^1H and ^{13}C NMR spectroscopy, due to the stereogenic center in the dmthqa ligand. Additionally, two signals arising from the *tert*-butylimido ligands were also observed, due to different *trans* donor ligands (*e.g.*, NMe_2 vs N_{pyr}). The proposed formula of **3b** was also confirmed using combustion analysis.

Following the isolation of **2b** and **3b**, we attempted to prepare two additional rigid analogues of *N,N'*-chelating ligands we used previously. First, 5,6-dihydro-*N*-(*tert*-butyl)-8-quinolinamine (dhtbqa), a hitherto unknown compound, was prepared from the condensation of 6,7-dihydro-5H-quinoline-8-one with *tert*-butylamine at 110 °C over 8 days. Unfortunately, dhtbqa was found to exist as its enamine tautomer, and treatment of it with $(^tBuN)_2MoCl_2$·dme led to an intractable mixture, presumably due to protonation of the imido ligands. Attempts to alkylate the *α*-position of dhtbqa,[16] to prevent the formation of the enamine tautomer, were unsuccessful. Finally, no reaction was observed between (*N,N'*-di-*tert*-butyl)phenathrene-9,10-diimine[17] (a rigid analogue of 1,4-di-*tert*-butyl-1,3-diazabutadiene), and $(^tBuN)_2MoCl_2$·dme, likely due to steric congestion of the four *tert*-butyl groups.

The solid-state structures of $(^tBuN)_2MoCl_2$·tmchd (**2b**) and $(^tBuN)_2MoCl_2$·dmthqa (**3b**) were also examined using single-crystal X-ray crystallography (**Figure 3**) to compare the structures to the non-rigid analogues (*e.g.*, **2a** and **3a**). In both cases the metal centers are octahedral with *trans* disposition of the chlorides, with Cl−Mo−Cl angles of 167.35(13) and 164.21(12)° for **2b** and **3b**, respectively. Additionally, the neutral ligands (tmchd for **2b** and dmthqa for **3b**) adopt a κ_2-coordination to metal, both of which bind *trans* to the *tert*-butyl imido ligands. In both cases the imido bond angles (Mo−N−C) are nearly linear (164.9(6)° for **2b** and 167.2(9)° & 168.2(10)° for **3b**), and the slight deviation between the two is most likely due to crystal packing interactions,[18,19] and not the different electronic demands of the molybdenum centers.[18,20] Expectedly, the tmchd ligand in **2b** maintains its *(1S, 2S)*-stereochemistry upon coordination to the metal center. Finally, despite the dmthqa ligand being racemic, only crystals containing the *8S*-stereoisomer of dmthqa in **3b** were observed.

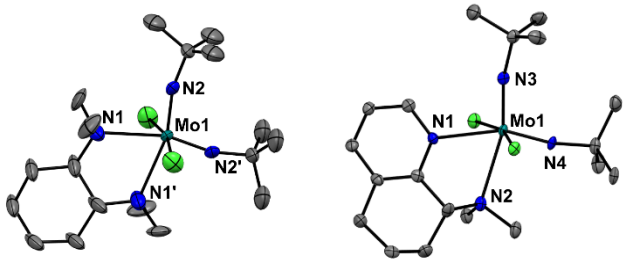

Figure 3. Solid-state structures of $(^tBuN)_2MoCl_2$·tmchd (**2b**, left) and $(^tBuN)_2MoCl_2$·dmthqa (**3b**, right). Half of **2b** was generated by symmetry. Thermal ellipsoids are drawn at the 50% probability level and hydrogen atoms have been omitted for visual clarity.

Table 1. Structural properties of (^{t}BuN)$_2$MoCl$_2$·L compounds highlighting the structural similarities between the rigid and non-rigid compounds. The decomposition temperature (measured by DSC) and the calculated free energy of ligand dissociation are also shown.

compound	ligand	Bite Angle N−Mo−N / °	Mo−N(*1/2*)	Buried Volume,[21] %V_{bur}	T_D / °C	BDFE[b], ΔG / kJ·mol^{-1}
1a	bpy	67.72(2)	2.3733(7), 2.3761(6)	28.3	272	87.9 (46.2)[c]
1b	phen	68.7(2)	2.374(6), 2.389(7)	27.9	303	83.6
2a	tmeda	71.7(2)	2.525(7), 2.556(7)	33.3	174	74.2 (21.5)[c]
2b	tmchd	71.8(3)	2.504(8)[a]	34.8	195	89.8
3a	dmampy	67.81(5)	2.3669(16), 2.5261(16)	31.1	200	79.5 (35.7)[c]
3b	dmthqa	67.3(4)	2.384(10), 2.523(12)	31.3	238	80.6
5	2-Phpy		2.341(4)	24.2	169	22.4

[a] Half of the molecule was generated by symmetry. [b] DLPNO-CCSD(T)/def2-TZVPP//r^{2}SCAN-3c. [c] BDFE starting from the κ_1-complex.

Comparing the structures of the rigid ligands (phen, tmchd, and dmthqa) to the non-rigid ligands (bpy, tmeda, and dmampy) many similarities are observed (**Table 1**). Firstly, the Mo−N(chelate) bond lengths are quite similar within a ligand class (*e.g.*, comparing bpy in **1a** to phen in **1b**). Additionally, the rigid ligands have similar bite angles as their non-rigid analogues (**Table 1**), which result in nearly identical buried volumes (%V_{bur}) within a ligand class. Combined these results suggest the steric and the electronic effects at the metal center are similar, regardless of the backbone of the ligand.

Hirshfeld analyses[22,23] also revealed similar intermolecular interactions within a ligand class (see SI). This suggests that the increased rigidification of a ligand does not drastically change the intermolecular interactions within the crystalline material. Therefore, the assumption is made that any additional thermal stability provided by ligand rigidification (*vide infra*) is not attributed to additional stabilizing intermolecular interactions.

After preparing the new rigidified compounds (**2b** and **3b**) we sought to explore their thermal properties. Using thermogravimetric analysis (TGA, see SI), both compounds exhibited moderate volatility, and had similar onset of volatilization temperatures (T_{onset}) as their non-rigid analogues (140 °C for **2a**[12] and 154 °C for **2b**; 150 °C for **3a**[12] and 174 °C for **3b**). Differential scanning calorimetry (DSC, see SI) was then used to measure the thermal stabilities of these compounds. In both cases the rigid complexes (**2b** and **3b**) had increased onset of decomposition temperatures (T_D) compared to **2a** and **3a** (**Table 1**). This is in line with what we observed between the bpy and phen ligands in **1a** and **1b**, and highlights increased rigidity in the ligand framework increases the barrier for thermal decomposition. Although the rigid analogues (**2b** and **3b**) are less volatile than the flexibile analogues (**2a** and **3a**), their increased thermal stabilitiy allows the use of higher temperature deposition processes, and more importantly serves as models to aid in our understanding of their thermal mechanisms.

We have previously shown that the bond dissociation free energy (BDFE) of chelating ligands has good correlation with their T_D for the class of (^{t}BuN)$_2$MoCl$_2$·L (L = neutral, *N,N'*-chelating ligand).[6] The uncoordinated (^{t}BuN)$_2$MoCl$_2$ complex then underwent further thermal decomposition.[6] This correlation was accurate when starting from the pentacoordinate, κ_1-complexes, which are accessed through their low energy isomerizations from their hexacoordinate, κ_2 ground states. The rigid ligands used in the new complexes (**1b**, **2b**, and **3b**) cannot access a κ_1-coordination, potentially leading to their increased T_D.

To gain insight into the mechanistic differences of the ligand dissociation between rigid and non-rigid ligands, we experiementally measured the activation barriers for the ligand dissociation. In this experiment, (AdN)$_2$MoCl$_2$·tmeda (**4a**)[12] and (AdN)$_2$MoCl$_2$·tmchd (**4b**) (see SI for synthetic details) were used as models for **2a** and **2b**, respectively. This is because in the case of **2a** and **2b**, the compounds are volatile, and thus we could not deconvolute ligand dissociation, from volatilization. In constrast, **4a** and **4b** are not volatile, and loss of the ligand, leading to (AdN)$_2$MoCl$_2$ is clearly observed in the TGA curve.

Using isothermal TGA experiments we were able to determine the rate of ligand dissociation from the metal complexes at different temperatures. In the case of **4b** an Arrhenius plot (**Figure 4**) revealed an activation energy (80.9±9.8 kJ·mol^{-1}) that corresponds to the calculated $\Delta G^{\ddagger}$ of 88.5 kJ·mol^{-1} (DLPNO-CCSD(T)/def2-TZVPP//r^{2}SCAN-3c) for the dissociation of tmchd from the hexacoordinate κ_2-complex **4b**, to (AdN)$_2$MoCl$_2$. In contrast, the much lower

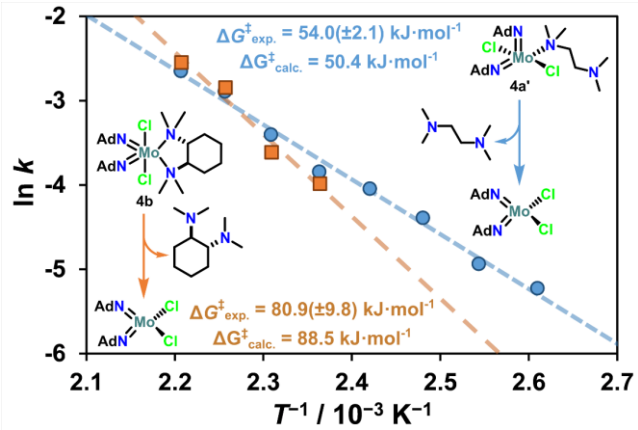

Figure 4. Arrhenius plot for the bond dissociation reaction of tmeda or tmchd from **4a** (blue circles) and **4b** (orange squares), respectively. Rate constants were obtained from the rate of moss-loss during isothermal TGA experiments.

activation energy for **4a** (54.0±2.1 kJ·mol^{-1}) corresponds to the calculated $\Delta G^{\ddagger}$ of 50.4 kJ·mol^{-1} for the dissociation of tmeda

from the pentacoordinate intermediate $(AdN)_2MoCl_2(\kappa_1$-tmeda) (**4a'**), to $(AdN)_2MoCl_2$. Eyring analyses for these transformations also revealed large positive $\Delta S^{\ddagger}$ values, confirming this process corresponds to a dissociative mechanism (see SI).

Clearly in the case of flexible ligands, κ_1-complexes appear to preferentially form. This is further emphasized by a computational relaxed potential energy surface (PES) scan where changes to the Mo−N(chelate) bond length was probed (**Figure 5**). In all cases, the flexible ligands do form stable κ_1-complexes (see SI for more examples). When the Mo−N bond lengthened in the complexes containing rigid ligands, such intermediates are not observed, instead the bidentate ligand undergoes a concerted dissociation, resulting in higher activation barriers for ligand dissociation (**Figure 5**).

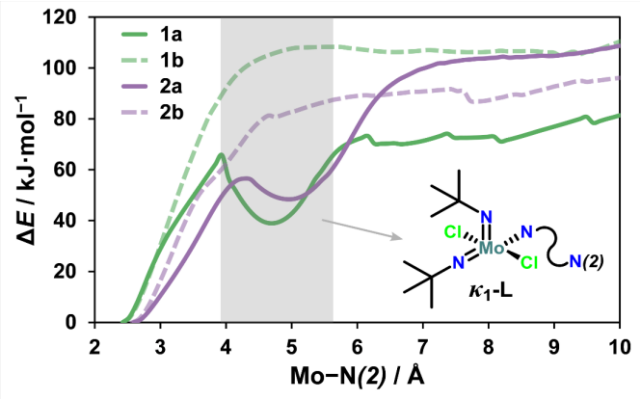

Figure 5. Relaxed potential energy surface scan for lengthening one Mo−N(chelate) bond in $(^tBuN)_2MoCl_2$·L. The inset shows the formation of the metastable κ_1-intermediates. Scans were performed at the r^{2}SCAN-3c level of theory, with a step size of 0.1 Å and optimizations performed after each step. The PES of other complexes can be found in the SI.

We also performed a PES scan of a complex that incorporates an anionic ligand that we previously described,[8] $(^tBuN)_2Mo(PyrIm)_2$ (PyrIm = *N*-2-(*tert*-butyliminomethyl)-pyrrolato), and showed the same process of rigidification also increases the activation barrier for ligand disociation, and prevents the formation of a κ_1-intermediate (see SI). This highlights a broader and more applicable application to this process of ligand rigidification because of the number of *N,N'*-chelating anionic ligands that are used in vapor deposition precursors; $(^tBuN)_2WCl_2$·L and $(^tBuN)NbCl_3$·L complexes also followed this trend (see SI).

The pentacoordinate κ_1-complexes appear to be metastable, and active intermediates for the decomposition of this class of molecule. Therefore, we were curious if we could isolate a model of this complex for further investigation. We have recently reported a chromium analogue of these compounds, $(^tBuN)_2CrCl_2$·dad (dad = 1,4-di-tert-butyl-1,3-diazabutadiene),[24] that was isolated and characterized as a κ_1-complex in the solid-state, but we have not observed such complexes for molybdenum.

However, sublimation of $(^tBuN)_2MoCl_2$·2py (py = pyridine) results in $(^tBuN)_2MoCl_2$·py with the loss of one equivalent of pyridine,[13] but, we were unable to obtain X-ray qualitiy crystals of that compound. This observation led us to use 2-phenylpyridine (2-Phpy), which is structurally similar to 2,2'-bipyridine (bpy). Direct treatment of $(^tBuN)_2MoCl_2$·dme with 2-Phpy led to the isolation of $(^tBuN)_2MoCl_2$·(2-Phpy) (**5**) (see SI for details). Analysis of the crystal structure of **5** revealed a square pyramidal (τ_5 = 0.07),[25] pentacoordinate complex, and is isostructural with the calculated structure of $(^tBuN)_2MoCl_2$·(κ_1-bpy) (**1a'**), with a root-mean-square deviation of 0.019 Å (**Figure 6**).

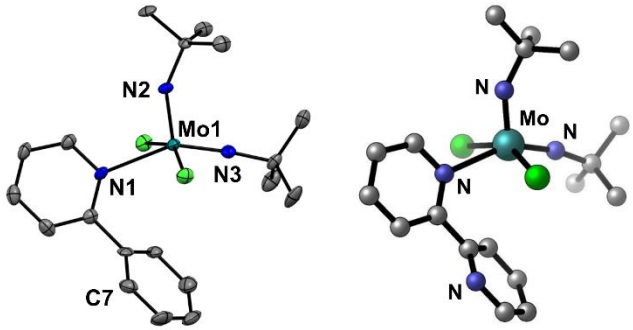

Figure 6. Solid-state structure of $(^tBuN)_2MoCl_2$·(2-Phpy) (**5**, left) and the optimized structure of $(^tBuN)_2MoCl_2$·(κ_1-bpy) (**1a'**, right). Hydrogen atoms have been omitted from both structures for visual clarity. Geometry optimizations were performed at the r^{2}SCAN-3c level of theory.

Compound **5** has a very low T_D (**Table 1**), which is equivalent to the T_D of $[(^tBuN)Mo(\mu\text{-}N^tBu)Cl_2]_2$,[13] further suggesting that κ_1-complexes are direct intermediates to the dissociation of the bidentate ligands, therefore the formation of these intermediates is likely the rate determining step in many of these thermolysis reactions.

Here we have provided further insight into the mechanism of thermolysis of the class of $(^tBuN)_2MoCl_2$·L compounds by investigation of monodentate vs. chelate dissociation of the κ_2-L ligand; the rate determining step of thermal decomposition of this class of compounds. By using ligands that are rigid, the chelating ligand is unable to undergo isomerization to a κ_1-intermediate, thus increasing the BDFE of the ligands. This method directly increases the thermal stability of these compounds, increasing their stability at significantly higher temperatures. This method could be further used to to control the stability of CVD precursors, for the development of new vapor-phase deposition processes.

ASSOCIATED CONTENT

Supporting Information

Supporting Information is available.

Experimental details, synthesis of compounds, NMR spectra, TGA plots, DSC curves, additional crystallographic images, and computational data (PDF)

Accession Codes

CCDC 2335568-233571 contain the supplementary crystallographic data for this paper. These data can be obtained free of charge via www.ccdc.cam.ac.uk/data_request/cif, or by emailing data_request@ccdc.cam.ac.uk, or by contacting The Cambridge Crystallographic Data Centre, 12 Union Road, Cabridge CB2 1EZ, UK; fax: + 44 1223 336033.

AUTHOR INFORMATION

Corresponding Author

*Email: Michael.land@dal.ca

Present Address

[#]Department of Chemistry, Dalhousie University, Halifax, Nova Scotia, Canada

ORCID

Michael A. Land: 0000-0001-5861-242X
Kieran G. Lawford: 0000-0002-1837-3150
Lara K. Watanabe: 0000-0002-0327-5611
Marshall Atherton: 0009-0004-1811-1945
Seán T. Barry: 0000-0001-5515-4734

Notes

The authors declare no competing financial interest.

ACKNOWLEDGMENTS

M.A.L. thanks the Natural Sciences and Engineering Research Council of Canada (NSERC) for funding through the Alexander Graham Bell CGS-D Scholarship, and the NSERC PDF program for support during manuscript preparation. K.G.L. thanks NSERC for funding through the CGS-M Scholarship. S.T.B. acknowledges NSERC for support through the Discovery Grants Program (RGPIN-2019-06213). We are also extremely grateful to Dr. Katherine Robertson of Saint Mary's University for her crystallographic expertise. Finally, we thank the Digital Research Alliance of Canada for providing computational facilities.

REFERENCES

(1) Coyle, J. P.; Kurek, A.; Pallister, P. J.; Sirianni, E. R.; Yap, G. P. A.; Barry, S. T. Preventing Thermolysis: Precursor Design for Volatile Copper Compounds. *Chemical Communications* **2012**, *48* (84), 10440.

(2) Barry, S. T. Amidinates, Guanidinates and Iminopyrrolidinates: Understanding Precursor Thermolysis to Design a Better Ligand. *Coord Chem Rev* **2013**, *257* (23–24), 3192–3201.

(3) Wu, J.; Li, J.; Zhou, C.; Lei, X.; Gaffney, T.; Norman, J. A. T.; Li, Z.; Gordon, R.; Cheng, H. Computational Study on the Relative Reactivities of Cobalt and Nickel Amidinates via β-H Migration. *Organometallics* **2007**, *26* (11), 2803–2805.

(4) Li, Z.; Gordon, R. G.; Pallem, V.; Li, H.; Shenai, D. V. Direct-Liquid-Injection Chemical Vapor Deposition of Nickel Nitride Films and Their Reduction to Nickel Films. *Chemistry of Materials* **2010**, *22* (10), 3060–3066.

(5) Beh, E. S.; Tong, L.; Gordon, R. G. Synthesis of 5,5-Bicyclic Amidines as Ligands for Thermally Stable Vapor Deposition Precursors. *Organometallics* **2017**, *36* (8), 1453–1456.

(6) Land, M. A.; Bačić, G.; Robertson, K. N.; Barry, S. T. Origin of Decomposition in a Family of Molybdenum Precursor Compounds. *Inorg Chem* **2022**, *61* (42), 16607–16621.

(7) Land, M. A.; Lomax, J. T.; Barry, S. T. Low-Temperature, Single-Source, Chemical Vapor Deposition of Molybdenum Nitride Thin Films. *Journal of Vacuum Science & Technology A* **2023**, *41* (5), 053403.

(8) Land, M. A.; Dimova, D. A.; Robertson, K. N.; Barry, S. T. Cut-and-Pasting Ligands: The Structure/Function Relationships of a Thermally Robust Mo(VI) Precursor. *Journal of Vacuum Science & Technology A* **2023**, *41* (1), 012403.

(9) Barry, S. T.; Gordon, P. G.; Vandalon, V. Common Precursors and Surface Mechanisms for Atomic Layer Deposition. In *Comprehensive Organometallic Chemistry IV*; Elsevier, 2022; pp 534–552.

(10) Samii, R.; Zanders, D.; Buttera, S. C.; Kessler, V.; Ojamäe, L.; Pedersen, H.; O'Brien, N. J. Synthesis and Thermal Study of Hexa-coordinated Aluminum(III) Triazenides for Use in Atomic Layer Deposition. *Inorg Chem* **2021**, *60* (7), 4578–4587.

(11) Brazeau, A. L.; Wang, Z.; Rowley, C. N.; Barry, S. T. Synthesis and Thermolysis of Aluminum Amidinates: A Ligand-Exchange Route for New Mixed-Ligand Systems. *Inorg Chem* **2006**, *45* (6), 2767–2767.

(12) Land, M. A.; Bačić, G.; Robertson, K. N.; Barry, S. T. Thermal Stability and Decomposition Pathways in Volatile Molybdenum(VI) Bis-Imides. *Inorg Chem* **2022**, *61* (12), 4980–4994.

(13) Land, M. A.; Robertson, K. N.; Barry, S. T. Ligand-Assisted Volatilization and Thermal Stability of Bis(Imido)Dichloro-molybdenum(VI) ([(t-BuN═)2MoCl2]2) and Its Adducts. *Organometallics* **2020**, *39* (7), 916–927.

(14) Dyer, P. W.; Gibson, V. C.; Howard, J. A. K.; Whittle, B.; Wilson, C. Four Coordinate Bis(Imido) Alkene Complexes of Molybdenum(IV): Relatives of the Zirconocene Family. *J Chem Soc Chem Commun* **1992**, *04* (22), 1666–1668.

(15) Description, A. G.; The, O. F. Eschweiler-Clarke Methylation. In *Comprehensive Organic Name Reactions and Reagents*; Wiley, 2010; pp 1009–1012.

(16) Huang, C.; Zhang, Y.; Liang, T.; Zhao, Z.; Hu, X.; Sun, W.-H. Rigid Geometry 8-Arylimino-7,7-Dimethyl-5,6-Dihydroquinolyl Nickel Bromides: Single-Site Active Species towards Ethylene Polymerization. *New Journal of Chemistry* **2016**, *40* (11), 9329–9336.

(17) Cherkasov, V. K.; Druzhkov, N. O.; Kocherova, T. N.; Shavyrin, A. S.; Fukin, G. K. N,N′-Disubstituted Phenanthrene-9,10-Diimines: Synthesis and NMR Spectroscopic Study. *Tetrahedron* **2012**, *68* (5), 1422–1426.

(18) Parkin, G.; Van Asselt, A.; Leahy, D. J.; Whinnery, L.; Hua, N. G.; Quan, R. W.; Henling, L. M.; Schaefer, W. P.; Santarsiero, B. D.; Bercaw, J. E. Oxo-Hydrido and Imido-Hydrido Derivatives of Permethyltantalocene. Structures of (η^5-C_5Me_5)2Ta(O)H and (η^5-C_5Me_5)2Ta(NC_6H_5)H: Doubly or Triply Bonded Tantalum Oxo and Imido Ligands? *Inorg Chem* **1992**, *31* (1), 82–85.

(19) Barrie, P.; Coffey, T. A.; Forster, G. D.; Hogarth, G. Bent vs. Linear Imido Ligation at the Octahedral Molybdenum(VI) Dithiocarbamate Stabilised Centre. *Journal of the Chemical Society, Dalton Transactions* **1999**, No. 24, 4519–4528.

(20) Ciszewski, J. T.; Harrison, J. F.; Odom, A. L. Investigation of Transition Metal−Imido Bonding in M(NBut)2 (Dpma). *Inorg Chem* **2004**, *43* (12), 3605–3617.

(21) Falivene, L.; Cao, Z.; Petta, A.; Serra, L.; Poater, A.; Oliva, R.; Scarano, V.; Cavallo, L. Towards the Online Computer-Aided Design of Catalytic Pockets. *Nat Chem* **2019**, *11* (10), 872–879.

(22) Spackman, M. A.; Jayatilaka, D. Hirshfeld Surface Analysis. *CrystEngComm* **2009**, *11* (1), 19–32.

(23) Spackman, P. R.; Turner, M. J.; McKinnon, J. J.; Wolff, S. K.; Grimwood, D. J.; Jayatilaka, D.; Spackman, M. A. CrystalExplorer: A Program for Hirshfeld Surface Analysis, Visualization and Quantitative Analysis of Molecular Crystals. *J Appl Crystallogr* **2021**, *54*, 1006–1011.

(24) Lawford, K. G.; Land, M. A.; Goodwin, E.; Robertson, K. N.; Barry, S. T. Synthesis, Characterization, and Single-Crystal X-Ray Structures of Refractory Metal Compounds as Precursors for the Single-Source Chemical Vapor Deposition of Metal Nitrides. *Inorg Chem* **2023**, *62* (51), 21061–21073.

(25) Addison, A. W.; Rao, T. N.; Reedijk, J.; van Rijn, J.; Verschoor, G. C. Synthesis, Structure, and Spectroscopic Properties of Copper(II) Compounds Containing Nitrogen–Sulphur Donor Ligands; the Crystal and Molecular Structure of Aqua[1,7-Bis(N-Methylbenzimidazol-2′-Yl)-2,6-Dithiaheptane]Copper(II) Perchlorate. *J. Chem. Soc., Dalton Trans.* **1984**, No. 7, 1349–1356.